

Space-Charge Effects in Field Emission*

J. P. BARBOUR, W. W. DOLAN, J. K. TROLAN, E. E. MARTIN, AND W. P. DYKE
Physics Department, Linfield College, McMinnville, Oregon

(Received June 8, 1953)

A progressive reduction of the observed field current below values expected from the empirical law for increasing values of the potential is attributed to space charge. The current density expected in the presence of space charge is calculated from the Fowler-Nordheim field emission theory using values of the cathode electric field obtained from a solution of Poisson's equation for plane electrodes with boundary conditions appropriate to field emission. The result is a generalization of Child's equation, and is asymptotic to it when the applied potential is large compared with the value required for appreciable field emission. Current densities predicted by the theory are compared with experimental values obtained for several values of the work function by use of the clean tungsten and the barium-on-tungsten emitting surfaces in high vacuum.

The Fowler-Nordheim theory correctly predicts the observed average current density from clean tungsten for densities in the range from 2 amp/cm² to 4×10⁷ amp/cm², thus extending a previous test of the theory which was limited to current densities less than 6×10⁶ amp/cm². Significant features of the electron emission pattern observed at high current densities are explained as effects of space charge.

INTRODUCTION

THE present paper concerns a quantitative study of the effects of space charge on the field emission of electrons from metals in high vacuum. This study was suggested by an earlier experiment¹ in which there was observed a reduction of field current below the values predicted by the empirical law² for increasing values of applied potential. The effect was observed only at current densities J greater than J_c where $J_c = 6 \times 10^6$ amp/cm² for a typical emitter. It was shown that the electron charge density near the tungsten emitter appreciably alters its surface electric field when $J \geq J_c$; however, a detailed study applicable at larger densities was not made at that time.

The stable emission of field current densities about two orders of magnitude larger than J_c ^{1,3,4} encourages a number of associated studies, each of which requires for its interpretation knowledge of the magnitude of the cathode electric field. At such current densities, space charge precludes use of previously described methods for the calculation of that field;⁵ however, that calculation has been accomplished in the present work through a solution of Poisson's equation with space charge included. This work thus extends the preliminary calculations of Stern, Gossling, and Fowler,⁶ who found no experimental evidence for a space-charge effect in field emission at the lower current densities then available.

The present study permits extension of the com-

parison between experiment and the wave mechanical field-emission theory^{7,8} to a current density of 4×10⁷ amp/cm², an earlier comparison¹ being limited at the value of J_c noted above; while current densities larger than 4×10⁷ amp/cm² are emitted stably, resistive heating⁴ of the emitter then precludes use of the theory⁷ which is applicable only at low temperatures.

Significant features of the field-emission pattern observed in a Mueller type projection tube at large current densities are herein explained as effects of space charge.

Child's equation, relating thermal emission current density to voltage, and calculated on the assumption of zero cathode field, is shown not applicable to field emission except when the applied voltage is large compared with the value V_c , corresponding to the current density J_c .

Knowledge of the cathode electric field in the presence of space charge will be useful in further analysis of the field-emission initiated vacuum arc^{3,4} and of the emission of electrons from metals at high temperatures and high fields, presently under study.

THEORETICAL DEVELOPMENT

Determination of the voltage necessary for a given cathode electric field in the presence of space charge requires a solution of Poisson's equation with boundary conditions appropriate to field emission. These conditions are:

- (1) a value of the cathode electric field in the range $10^7 < F < 10^8$ v/cm,
- (2) electrode geometries which in a typical case include a conical emitter with a hemispherical tip⁵ and an anode which is either spherical or plane, and

⁷ A. Sommerfeld and H. Bethe, *Handbuch der Physik* (J. Springer, Berlin, 1933), Vol. XXIV, No. 2, p. 441.

⁸ R. H. Fowler and L. W. Nordheim, Proc. Roy. Soc. (London) A119, 173 (1928).

* This work was supported principally by the U. S. Office of Naval Research; in part it was supported by the U. S. Air Force.

¹ W. P. Dyke and J. K. Trolan, Phys. Rev. 89, 799 (1953).

² R. A. Millikan and C. C. Lauritsen, Proc. Nat. Acad. Sci. 14, 1 (1928).

³ Dyke, Trolan, Martin, and Barbour, Phys. Rev. 91, 1043 (1953).

⁴ Dolan, Dyke, and Trolan, Phys. Rev. 91, 1054 (1953).

⁵ Dyke, Trolan, Dolan, and Barnes, J. Appl. Phys. 24, 570 (1953).

⁶ Stern, Gossling, and Fowler, Proc. Roy. Soc. (London) A124, 699 (1929).

(3) a nonuniform current density distribution at the cathode.⁹

The mathematical difficulties introduced by the foregoing boundary conditions were sufficient to preclude an exact solution of the problem by use of available methods. Attention was therefore turned to an approximate solution which led to good agreement with experiment.

Two limiting cases in which one would expect an effect of space charge on field emission were recognized: (a) when the space charge in transit between electrodes was an appreciable fraction of the total charge on one electrode, and (b) when the space charge near a small area on the cathode surface was an appreciable fraction of the charge on that area. The latter was shown to be applicable in experiments reported in reference 1. In that work, the field emission of electrons from clean tungsten was not detectably affected by space charge until the average current density at the cathode exceeded the critical value J_c noted above. It was shown that for $J=J_c$ sufficient space charge was present within the distance $s=2\times 10^{-6}$ cm from the emitter surface to alter sufficiently the cathode electric field to account for the deviation of observed current from the theoretically expected value.

The foregoing suggests that it is reasonable to approximate the electrode geometries as planes for the present theoretical study of the space-charge problem, since the value of s noted above is an order of magnitude less than the radius of curvature of the smallest hemispherical emitter commonly used. It was possible to use experimental values of both the applied potential and the cathode field (when space charge was negligible) in the calculations by choice of a spacing between planes of the order of 10^{-4} cm, i.e., about 100s or about 10 emitter radii. This method is roughly equivalent to the assumption that space charge at distances from the cathode larger than 10^{-4} cm has negligible effect on the emission, which assumption appears justified under the present conditions from the foregoing and from the agreement between experiment and theory which follows. Plane electrodes were also used in the preliminary study of Stern, Gossling, and Fowler.⁶

The form taken by Poisson's equation for plane metal electrodes and a negative space charge is

$$d^2V/dx^2 = kJV^{-\frac{1}{2}}, \quad (1)$$

where V is a function of x alone, the x axis is normal to the electrode planes with $x=0$ and $V=0$ at the cathode, and $k=2\pi(2m/e)^{\frac{1}{2}}$, all units in esu. If solved for the boundary condition of zero cathode field, which is usually assumed applicable in thermionic emission, Eq. (1) leads to Child's equation,

$$J = (4/9kx^2)V^{\frac{3}{2}}. \quad (2)$$

For field emission the cathode surface field has a non-

vanishing value F_0 , and the integration of Eq. (1), which is straightforward, differs from that of the thermionic case and yields the relation

$$(2kJV^{\frac{3}{2}} - F_0^2)(4kJV^{\frac{3}{2}} + F_0^2)^{\frac{1}{2}} = 6k^2J^2d - F_0^3, \quad (3)$$

where d is the spacing between electrodes. This equation is equivalent to that obtained by Stern, Gossling, and Fowler⁶ who carried the work no further than this point.

It would be desirable to eliminate F_0 from this equation in order to express J as a function of V , but this arrangement is mathematically inconvenient. It is more satisfactory to eliminate J between Eq. (3) and the following expression which is the fundamental Fowler-Nordheim field-emission equation,^{7,8}

$$J = 1.54 \times 10^{-6} (F_0^2/\phi) \exp[-6.83 \times 10^7 \phi^{\frac{3}{2}} f(\gamma)/F_0], \quad (4)$$

where ϕ is the work function in ev, J is in amp/cm², F_0 is in v/cm, and $f(\gamma)$ is Nordheim's elliptic function of the variable $\gamma = 3.79 \times 10^{-4} F_0^{\frac{1}{2}}/\phi$, presently accepted values of the physical constants being used. Calculations based on Eq. (4) have made use of a recent correction¹⁰ in the values of Nordheim's function. This equation is not explicitly solvable for F_0 , but it is easy to eliminate J between Eqs. (4) and (3), after making appropriate alterations in Eq. (3) to permit the use of practical units instead of esu. If Eq. (4) is abbreviated to $J = cF_0^2 \exp(-b/F_0)$, the result of the elimination is

$$4kcV^{\frac{3}{2}} \exp(-b/F_0) - 3V = 9k^2c^2F_0^2d^2 \exp(-2b/F_0) - 3F_0d. \quad (5)$$

Under the foregoing assumptions, this is the general equation for space-charge limited field emission, yielding with the aid of Eq. (4) the value of current density at any given potential.

At small values of F_0 , the positive terms of Eq. (5) are negligible, and the relation reduces to $V = F_0d$ as expected. At much larger values the negative terms are negligible, and the equation reduces to Eq. (2). Over the intermediate range, further investigation is desirable. For this purpose a numerical form of the coefficients of Eq. (5) is obtained

$$(3.90 \times 10^{-1}/\phi)V^{\frac{3}{2}} \exp(-b/F_0) - V = (25.8 \times 10^{-2}/\phi^2)F_0^2d^2 \exp(-2b/F_0) - F_0d. \quad (6)$$

In the calculation of the curves discussed below, the exponentials of Eq. (6) are expressed with base 10 for convenience in computation.

The electrode spacing d , needed in Eq. (6), must be chosen in such a way as to give a theoretical surface field F_0 (in the absence of space charge) equal to the experimentally observed field for a given value of the applied potential. This is accomplished by noting that $F = V/d$ for the plane electrodes, while $F = \beta V$ in the experimental geometry; the factor β , which is constant for a given emitter, is obtained either through Eq. (6)

⁹ W. P. Dyke and J. K. Trolan, Phys. Rev. **85**, 391 (1952).

¹⁰ Burgess, Kroemer, and Houston, Phys. Rev. **90**, 515 (1953).

of reference 1 or Eq. (3) of reference 5, the latter by use of electron micrographs. The desired equality between theoretical and experimental surface fields in the absence of space charge is therefore obtained by substituting $1/\beta$ for d in Eq. (6).

The curve ACD of Fig. 1 was constructed by plotting J , as calculated¹¹ from Eq. (4) for a sequence of arbitrarily chosen values of F_0 , against V from Eq. (6) for the same values of F_0 . Substitution of any value of F_0 into Eq. (6) yields a numerical equation of the form $AV^{\frac{3}{2}} - V = B$. Although this might be solved explicitly as a cubic in $V^{\frac{3}{2}}$, the procedure is clumsy and it is easier to find the roots by approximation. As long as B is negative there are two roots for V , but only one of them is physically admissible, and the choice is made on the basis of continuity, beginning with $V=0$ when $F_0=0$.

The curve ACD , Fig. 1, is asymptotic to the curve

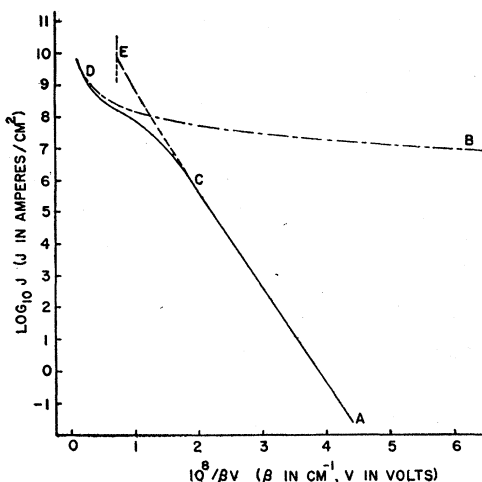


FIG. 1. Theoretical dependence of field current density J on applied voltage V . Curve ACE , Fowler-Nordheim theory without space charge; curve ACD , space-charge corrected theory; curve BD , Child's equation for comparison.

BD calculated from Child's Law [Eq. (2)]. Curve ACE results from the Fowler-Nordheim theory [Eq. (4)] if space charge is assumed negligible.

EXPERIMENTAL METHOD

Experimental field current-voltage relationships, required for comparison with the corresponding theoretical curves presented in the previous section, were obtained by the methods of references 1 and 3, with certain refinements noted in the following.

Field emission from cathode surfaces of various work functions, required for the comparison shown later in Fig. 7, was obtained from a tungsten cathode which had various partial surface coatings of barium.^{12,13} Since the

¹¹ W. W. Dolan, Phys. Rev. **91**, 510 (1953).

¹² E. W. Mueller, Z. Physik **108**, 668 (1938).

¹³ J. A. Becker, Bell System Tech. J. **30**, 907 (1951).

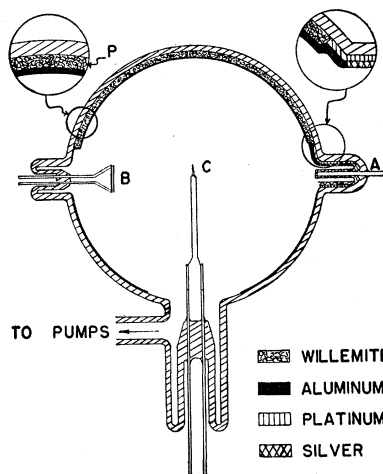


FIG. 2. Experimental tube. C , field cathode; P , aluminum backed phosphor anode; B , barium source; A , anode insul.

stability of the barium-on-tungsten surface during field emission at current densities approaching 10^8 amp/cm² as required for the present work had not been previously demonstrated, use was made of the electron emission pattern to monitor the cathode surface condition. Patterns were recorded simultaneously with the current-voltage relationship by the methods of references 1 and 3.

The experimental tube shown in Fig. 2, which was used for the present work, was similar to that described in Fig. 1 of reference 3 except for the present addition of the barium source B . That source, a Batalum strip, was heated resistively in order to evaporate barium onto the cathode C . The emission pattern was viewed on the aluminum backed phosphor (willemite) screen P . Fabrication of such anode screens is described elsewhere.³

The field cathode, a tungsten needle, was fabricated by previously described techniques.⁵ Residual pressures of chemically active gases in the experimental tube were less than 10^{-12} mm of Hg, and the total pressure was less than 10^{-10} mm of Hg at sealoff. Methods for obtaining and recording such pressures were described earlier.^{1,3}

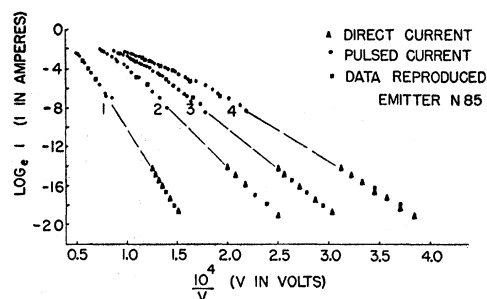


FIG. 3. Experimental field current-voltage data for Emitter N85. Curve 1, clean tungsten emitter; curves 2-4, tungsten with increasing surface coatings of barium.

EXPERIMENTAL RESULTS AND CONCLUSIONS

Current-voltage relationships for the combined direct current and pulsed operation of emitter *N*85 are shown in Fig. 3 in the usual form of $\ln I$ vs $10^4/V$, where I and V are current and voltage, respectively; curve 1 from clean tungsten, curves 2, 3, and 4 from correspondingly increased fractional surface coatings of barium-on-tungsten.

Stability of the cathode during the foregoing operation is argued from several lines of evidence. The reproducibility of the data, shown in Fig. 3, precluded irreversible changes in emitter geometry, work function,

and emitting area. The best evidence against reversible changes in those variables during a given run, for example, curve 2, Fig. 3, is found in the corresponding series of emission patterns of Fig. 4, taken at a wide range of currents during that run. The fine detail in the emission pattern is constant from pattern to pattern, indicating the stability of the barium coating during the present operation. In this regard it is convincing to compare the patterns *A* and *D* of Fig. 4, both of which were taken at a low direct current, respectively, before and after high-level pulse operation. The data from clean tungsten in curve 1 of Fig. 3 were reproduced

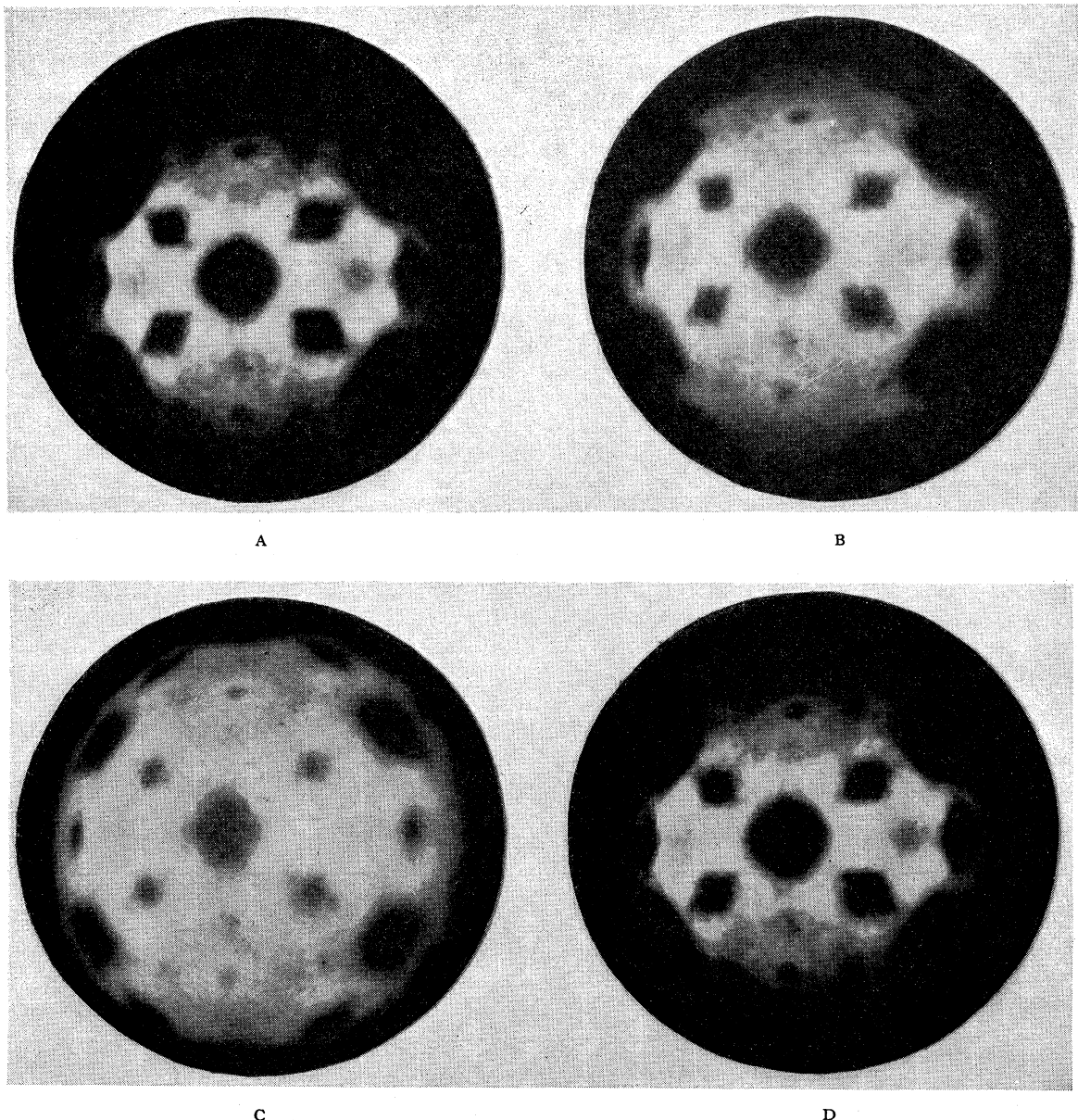


FIG. 4. Emission patterns at various currents, with constant work function $\phi = 3.19$, for emitter *N*85, corresponding to curve 2, Fig. 7.

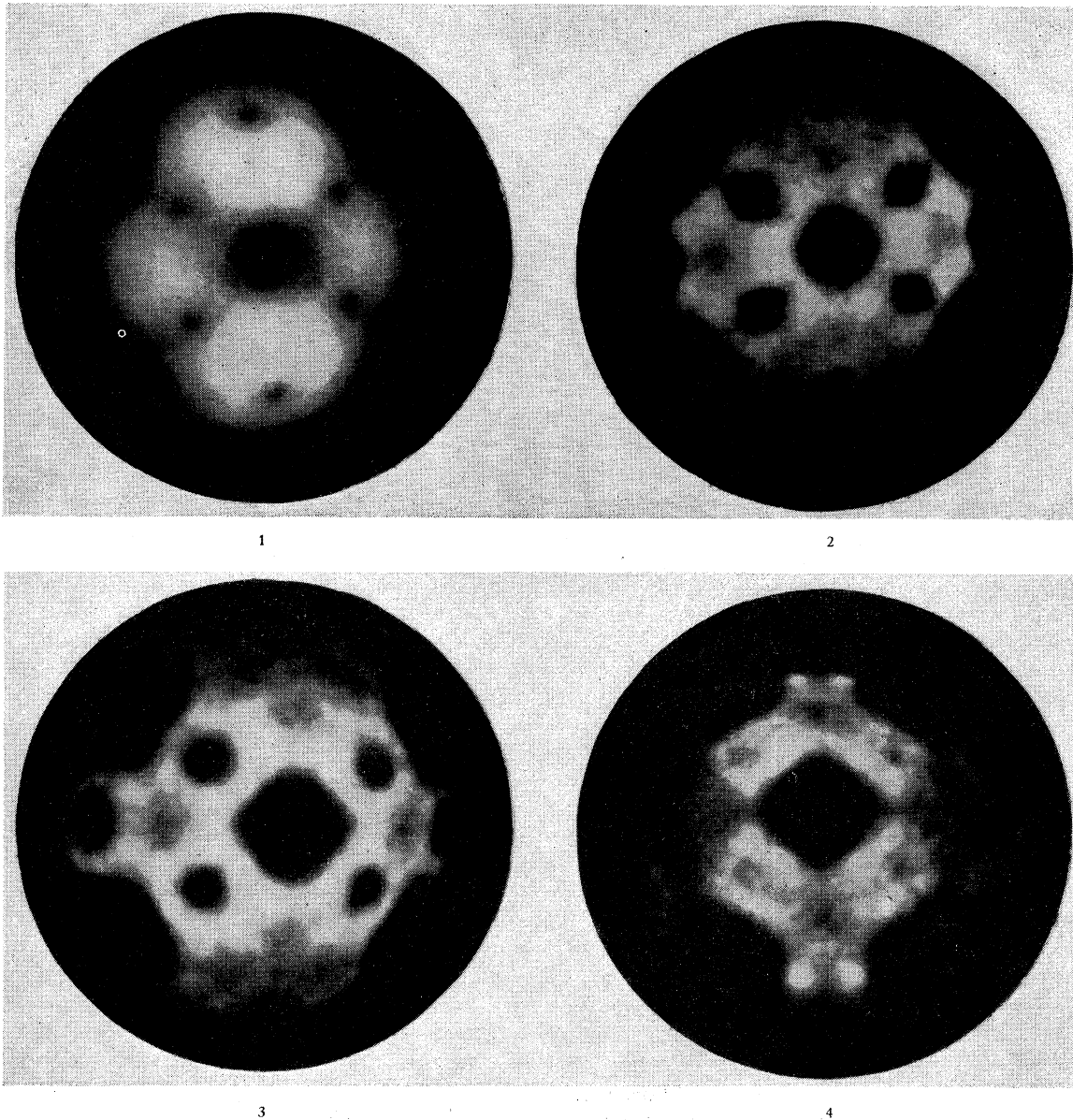


FIG. 5. Direct current emission patterns for emitter *N85*, with various average work functions as shown, corresponding to curves 1-4 of Fig. 7.

after the other data shown in the figure (the uncontaminated surface having been restored by heating) providing further evidence of cathode stability.

The series of emission patterns 1, 2, 3, and 4 of Fig. 5 were recorded at approximately the same direct current level (9×10^{-8} to 7×10^{-7} amps in various cases) corresponding to the curves 1, 2, 3, and 4 of Fig. 3. These patterns illustrate the various surface distributions of current density obtained from clean tungsten (pattern 1) and from increasing fractional coatings of barium-on-tungsten (patterns 2, 3, and 4). From these patterns the relative emitting areas may be estimated, and will be useful below.

The three emission patterns of Fig. 6, taken at a wide range of current densities, were obtained from the clean tungsten emitter *N85* and will be useful for comparison later with Fig. 8 which predicts the general features of these observed patterns.

The experimental data in Fig. 3 were compared with corresponding theoretical curves in Fig. 7. The latter were obtained from Eqs. (6) and (4) in the manner which led to Fig. 1. Values of the work function ϕ corresponding to the several curves of Fig. 3 were required. For curve 1, ϕ was assumed to be 4.5 ev, the average value for tungsten whose surface cleanliness was known from the emission pattern, Fig. 5a. For the

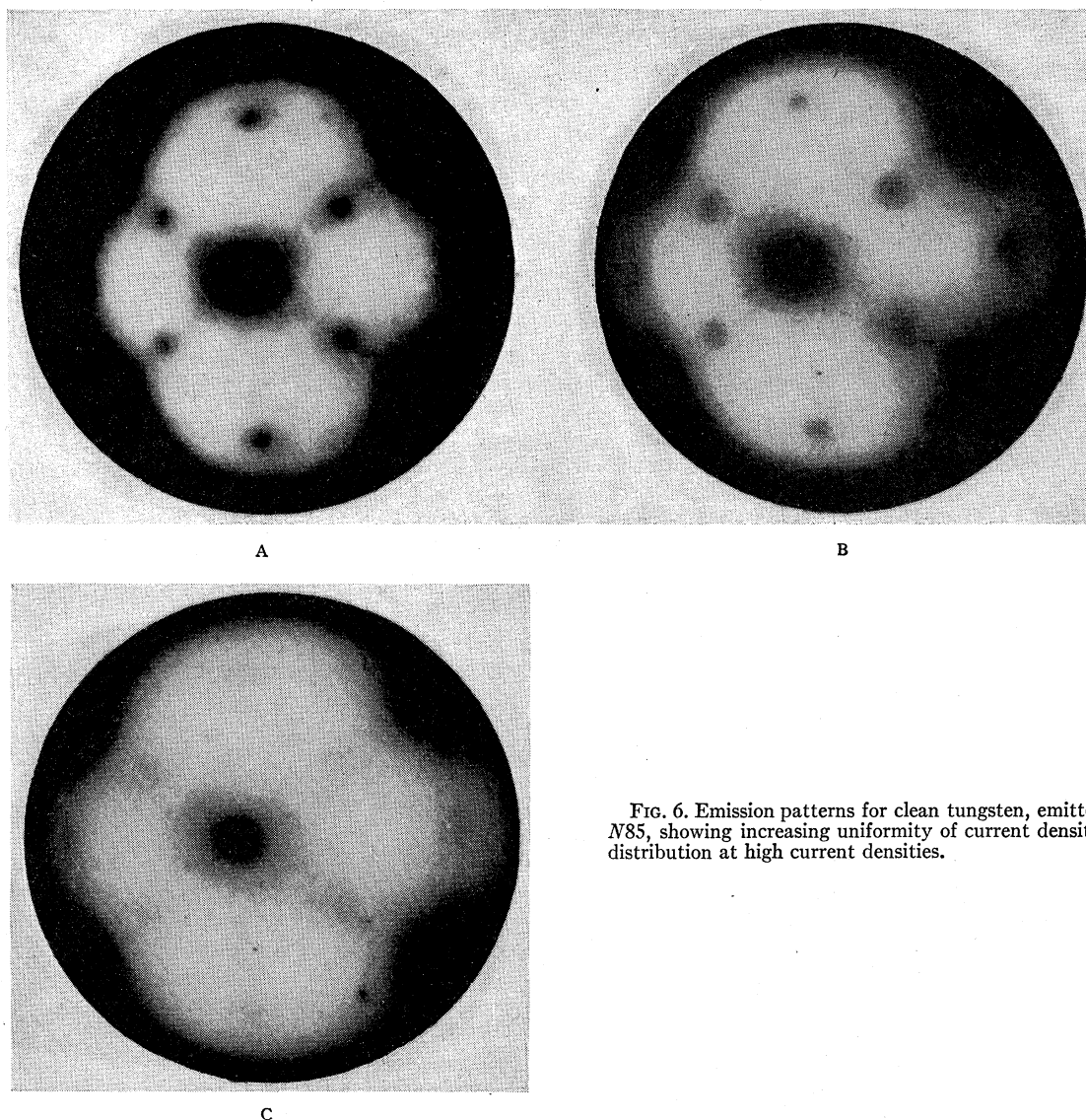


FIG. 6. Emission patterns for clean tungsten, emitter N85, showing increasing uniformity of current density distribution at high current densities.

other curves in Fig. 3, values of ϕ were obtained from the observed slopes of the curves (at low currents where space charge was negligible) and the known dependence of the slope on the work function.^{10,14} These values of ϕ were used in Eq. (6) to calculate the corresponding curves of Fig. 7. In the same figure are shown the experimental data from Fig. 3, replotted in the form $\log_{10} J$ vs $10^8/\beta_m V$ by the methods of reference 1. For this purpose use was made of the value of emitting area $A = 6.3 \times 10^{-9}$ cm² and the value $\beta_m = 4.0 \times 10^3$ cm⁻¹. The latter agrees, within the experimental error, with the value $\beta_0 = (3.7 \pm 0.6) \times 10^3$ cm⁻¹ calculated by the methods of reference 5. Knowledge of the emitter geometry, required for the calculation of both the area and β_0 , was obtained from electron micrographs of the emitter.

¹⁴ R. H. Haefner, Z. Physik 116, 604 (1940).

The agreement between experiment and theory shown in Fig. 7 is well within the experimental error, which is introduced primarily by the uncertainty in β_0 . Confining attention momentarily to curve 1 of that figure, it is seen that Eqs. (6) and (4) lead to the correct prediction of the observed average current density from clean tungsten in the range of current densities from 2 amp/cm² to 4×10^7 amp/cm², which extends the test of the theory from the previous¹ limit of 6×10^6 amp/cm².

Minor deviations between experiment and theory may be explained by two considerations involving small changes in the emitting area neglected above. First, the deviations at low current densities are consistent with the reasonable assumption that the emitting area is less for the partial coating of barium-on-tungsten than for clean tungsten. This assumption is confirmed by inspection of Fig. 3 (extrapolation of the linear portions of the curves to the infinite voltage axis

provides an approximate comparison of relative areas⁶). Second, the deviations at high current density which exhibit a consistent trend towards higher experimental densities than expected theoretically, are explained by the observation that the effective emitting area increased with the applied voltage. This effect is observed in Fig. 4 and was anticipated in Fig. 13 of reference 1. Correction for this effect would bring experiment and theory into closer agreement in Fig. 7.

It will be noticed from Fig. 7 that the current density required for a given space-charge effect decreases with the value of ϕ . This occurs for two reasons: (1) the electric field required for a given J decreases with ϕ and lower fields are less effective in removing space charge from the vicinity of the emitter surface; (2) at lower fields there is less induced charge on the cathode surface.

Certain changes in the surface distribution of current density from the clean tungsten field emitter are explained as an effect of space charge. The principal feature is an increase in uniformity of the distribution with increasing current density (Fig. 6), characterized by the gradual disappearance of the dark areas of the pattern which correspond to crystal faces of high work function.¹⁵ Such an effect is expected from Eqs. (6) and (4) when current density-voltage relationships are calculated for several faces of the tungsten monocrystal whose work functions are given by Nichols¹⁶ and by Smith.¹⁷ Relationships for the (211) crystal face ($\phi=4.65$ ev), the (310) crystal face ($\phi=4.35$ ev) and for the (110) crystal face (curve drawn for $\phi=5.0$ ev, a minimum value for this face whose value is not yet definitely established¹⁷) are shown in Fig. 8. The figure indicates that the current density levels from the three crystal faces would be indistinguishable at current densities $J \geq 10^8$ amp/cm².

Experimental verification of that prediction is seen from Fig. 6, which shows emission patterns from emitter N85 at a wide range of average values of current

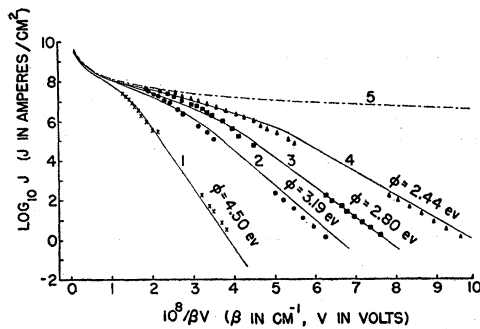


FIG. 7. Comparison of experimental data with space-charge field-emission theory (solid lines) for emitter N85. Curve 1, clean tungsten, curves 2-4, barium-on-tungsten as in Fig. 3; curve 5, Child's equation.

¹⁵ E. W. Mueller, *Z. Physik* **106**, 541 (1937).

¹⁶ M. H. Nichols, *Phys. Rev.* **57**, 297 (1940).

¹⁷ G. F. Smith, Abstracts of Field Emission Seminar, Linfield College, 1952 (unpublished).

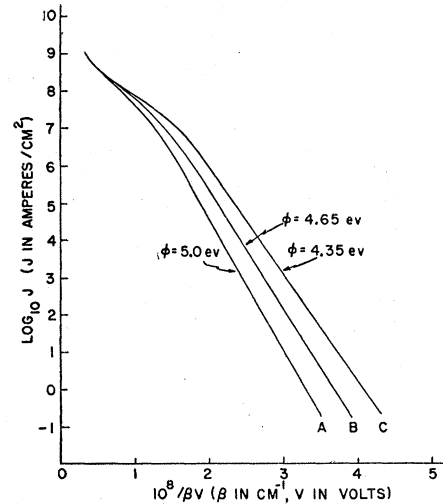
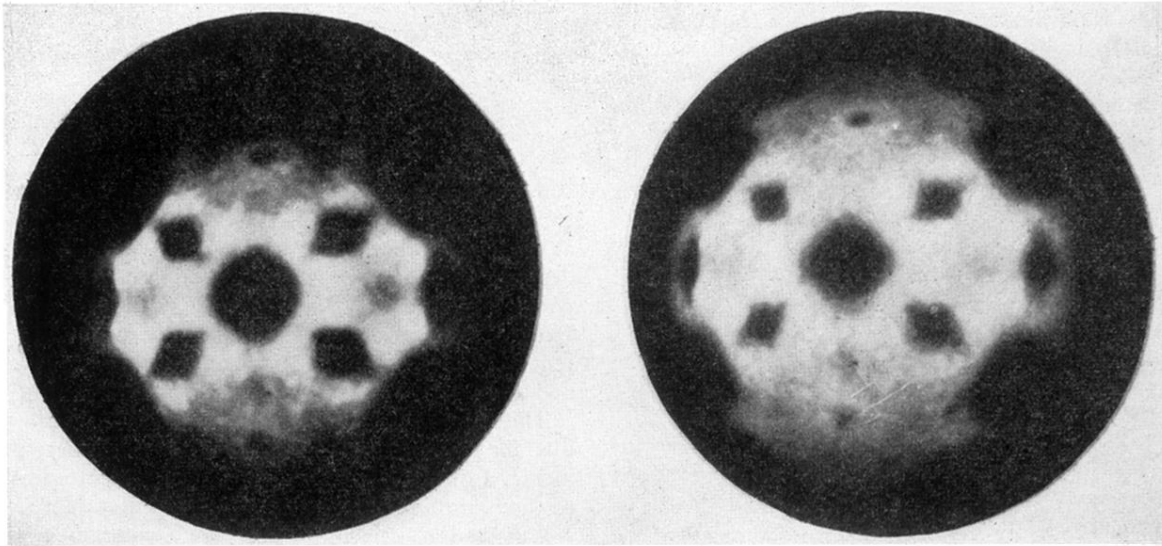


FIG. 8. Space-charge theory curves for work functions corresponding to various crystal faces of clean tungsten.

density recorded for the clean emitter during run 1 of Fig. 3. The several patterns in Fig. 6 correspond to average current densities as follows: (A) 16 amp/cm², (B) 3.5×10^6 amp/cm², (C) 1.4×10^7 amp/cm². Patterns (A) and (B) correspond roughly to the two extremities of the linear portion of the curves in Fig. 8, over which range space charge is negligible. The emission pattern detail is similar, and distinct in both patterns, indicating no marked change in current density distribution over the large indicated range of current densities, which observations are predicted by the curves of Fig. 8. On the other hand, the relatively small increase in average current density from pattern (B) to (C) caused marked changes in the pattern characterized by a more uniform current density distribution resulting from a relative increase in density at the (211) and (100) faces. This occurs at a current density near that for which curves B and C of Fig. 8 become indistinguishable; hence it is possible to explain the effect as due to space charge. On the other hand, the central dark region (110 face) is clearly distinguishable in all patterns of Fig. 6. This is expected from Fig. 8, curve A, which merges with curves B and C only at current densities $J > 10^8$ amp/cm², i.e., greater than those obtained in the present experiment, which as noted in the introduction was limited at 4×10^7 amp/cm² by the onset of appreciable resistive heating of the emitter.⁴ A further test of the predictions of Fig. 8 at higher current densities by use of an emitter with wide cone angle⁵ to minimize resistive heating⁴ is contemplated.

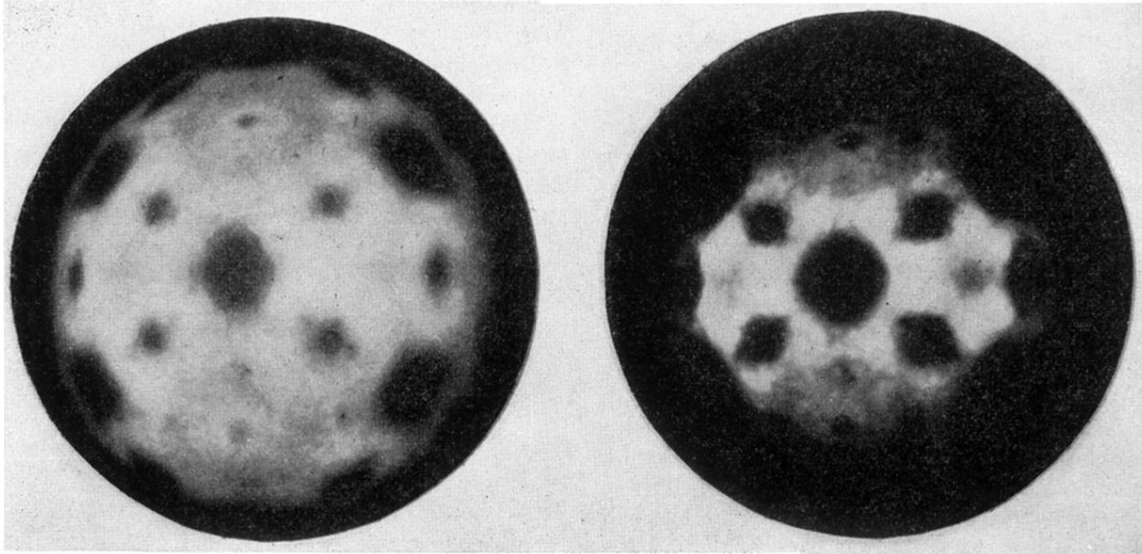
ACKNOWLEDGMENTS

Appreciation is extended to L. M. Perry, D. M. Barney, F. M. Collins, Professor J. L. Boling, and to student assistant Richard Perry for valuable technical assistance.



A

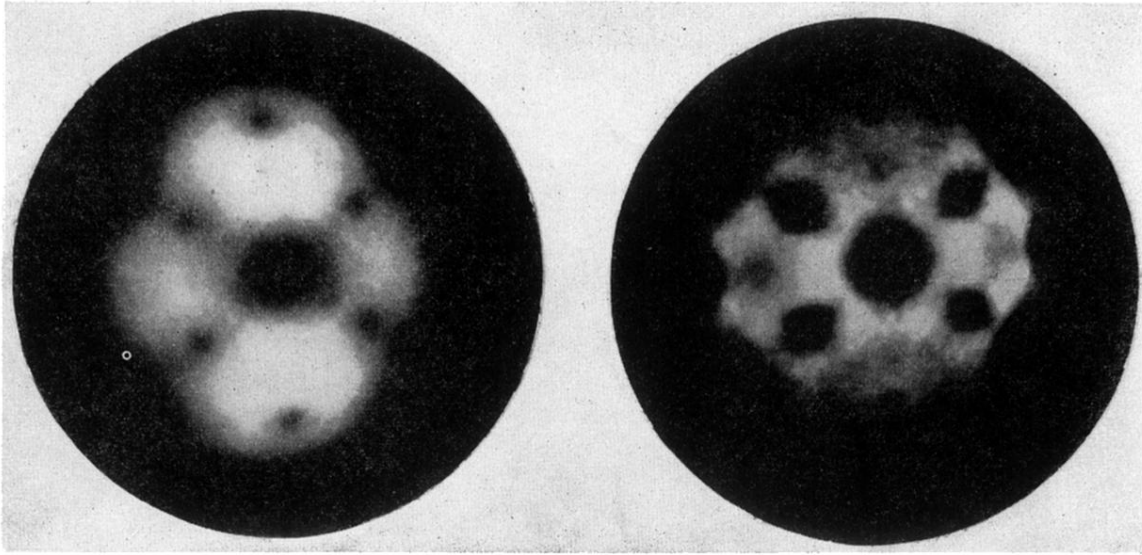
B



C

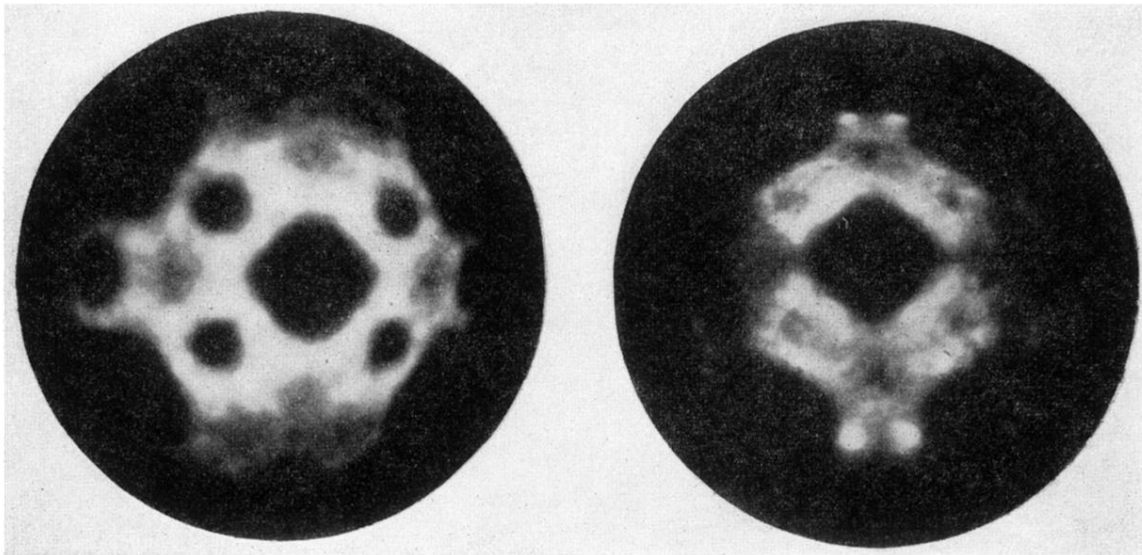
D

FIG. 4. Emission patterns at various currents, with constant work function $\phi=3.19$, for emitter N85, corresponding to curve 2, Fig. 7.



1

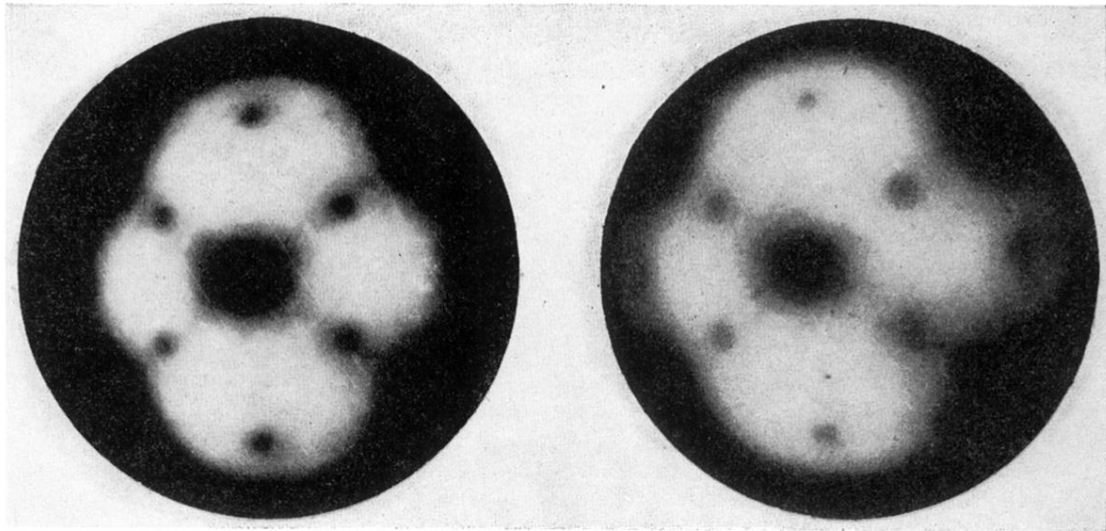
2



3

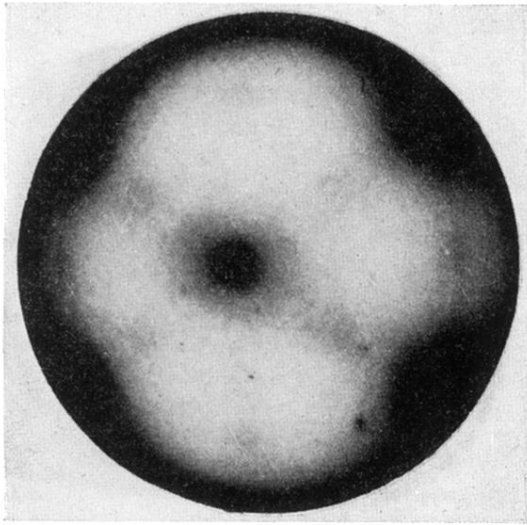
4

FIG. 5. Direct current emission patterns for emitter N85, with various average work functions as shown, corresponding to curves 1-4 of Fig. 7.



A

B



C

FIG. 6. Emission patterns for clean tungsten, emitter N85, showing increasing uniformity of current density distribution at high current densities.